NJC

ROYAL SOCIETY OF CHEMISTRY

COMMUNICATION

View Article Online
View Journal | View Issue

Check for updates

Cite this: *New J. Chem.*, 2024, 48, 9880

Received 20th March 2024,
Accepted 12th May 2024

DOI: 10.1039/d4nj01314j

rsc.li/njc

Static iodine loading comparisons between activated carbon, zeolite, alumina, aerogel, and xerogel sorbents†

Saehwa Chong, *[a] Brian J. Riley, [a] Karthikeyan Baskaran,[b] Sean Sullivan,[b] Luke El Khoury,[a] Krista Carlson,[b] R. Matthew Asmussen[a] and Matthew S. Fountain[a]

Different sorbents, including activated carbons, an Ag-aerogel, Ag-xerogels, an Ag-alumina, an Ag-zeolite, a Ag_2S-polyacrylonitrile composite, and a carbon foam were investigated for static $I_{2(g)}$ loading at 71 °C for 56 d followed by 4.7 d of desorption. The iodine loadings were 630–1249 mg g^{-1} for activated carbons and 87–744 mg g^{-1} for other sorbents.

Capture and immobilization of radioiodine is an ongoing concern for nuclear waste management.[1–3] Radioiodine includes ^{129}I and ^{131}I, which are fission products with half-lives ($t_{1/2}$) of 1.57×10^7 years and 8.02 days, respectively. Undesirable release of radioiodine is a public health and safety concern due to adverse effects on human health.[1–6] Different types of sorbents, including activated carbons,[7] aerogels,[8] xerogels,[9,10] zeolites,[11–13] and metal–organic frameworks (MOFs)[14] have been investigated for capturing gaseous iodine. In this study, the iodine loadings and adsorption rates of different commercial and developmental sorbents are compared. To evaluate several types of sorbents in a head-to-head competitive iodine capture experiment, twelve separate sorbents were used, including four activated carbons using six types, a zeolite, an alumina, three xerogels, a polymer composite, and a carbon foam.[15] The iodine loading capacities of the tested commercial activated carbons are not previously reported. Sample names and abbreviated names used in this paper are given in Table 1. The optical images of the sorbent materials before iodine uptake are shown in Fig. 1. All the Ag xerogels had similar appearances, and HTX-Ag is shown for example. The bottles of BAT37 (Donau Carbon) and BAT37-II (Donau Carbon) contained carbon sorbents and amorphous inert granules in a 70 : 30 mass ratio. The activated carbon sorbents in pellet forms included BAT37, BAT37-II, Des (Donau Carbon), Oxo (Donau Carbon), and Cab (NORIT) with similar cylindrical shapes of ≈3–4 mm diameter and ≈2–10 mm length; Dar (NORIT) had an irregular particle form of ≈2–10 mm. The IONEX (Ag-400, Molecular Products), AC-6120 (Clariant), and 75%Ag_2S–PAN (polyacrylonitrile) sorbents were in bead form with diameters of ≈1–3 mm, and the aerogel and xerogel sorbents had irregular shapes with sizes of 1–5 mm. The developmental sorbents including Ag-loaded aerogel,[8] xerogels,[9,10,16] PAN composite,[17] and carbon foam[18] were synthesized using similar methods as described in previous studies. All the commercial sorbent materials were used as received, and the sorbent materials except for carbon foam (CF) contained impregnated species of Ag, S, K, and/or I to aid chemisorption (Table 1). Two additional sorbents including Kombisorb BAS 55 (Donau Carbon) and AGC-50 CS-Si 1.05 (Resin Tech Inc.) were also tested, but their data were not included in this study due to inaccurate measurements with artifacts.

Iodine uptake experiments were performed to determine the iodine loadings of the sorbents. For these experiments, each sample was added to a pre-tared 5-mL glass vial; the masses were ≈1–3 g for activated carbons, Ag-400, AC-6120, and FA-Ag, whereas only ≈0.01–0.04 g were used for xerogels, carbon foam, and PAN due to the limited availability of these sorbents. Each sorbent was prepared in triplicate except for the xerogels and the PAN. All the prepared vials without lids were placed in 1-L PFA containers (Savillex) along with solid iodine pieces (Sigma-Aldrich, ≥99.99%) of ≈1 g L^{-1} to provide a saturated iodine environment. The PFA containers were placed in an oven at 71 ± 2 °C. At ≈24 h intervals, the PFA containers were removed from the oven and the lid was removed to degas for 10 min before measuring the sample masses. The gravimetric masses of the sorbents were measured daily for 16 d and then once a week until day 56. After 56 d, the PFA containers were placed back into the oven without iodine, and the sorbents were desorbed at 71 ± 2 °C for 114 h. The desorption process was performed to remove weakly bonded or physisorbed iodine. The appearances of the Ag-containing sorbents after iodine uptake are shown in Fig. 2a. The Ag-containing sorbents

[a] *Pacific Northwest National Laboratory, 902 Battelle Blvd, Richland, WA 99354, USA. E-mail: saehwa.chong@pnnl.gov*
[b] *University of Nevada, Reno, 1664 N Virginia St, Reno, NV 89557, USA*

† Electronic supplementary information (ESI) available. See DOI: https://doi.org/10.1039/d4nj01314j

Table 1 List of sorbent samples, abbreviated names, base materials, impregnation elements (or compounds), and forms. AC: activated carbon, C: carbon, Z: zeolite, A: alumina, AG: aerogel, XG: xerogel, and P: polyacrylonitrile, respectively. Pel and Par denote pellet and particle, respectively. References are provided where more details can be found for some of the sorbents

#	Sorbents	Abbr.	Base	Impreg.	Form	Ref.
1	Kombisorb BAT-37	BAT37	AC	S	Pel	15 and 19
2	Kombisorb BAT-II-37	BAT37-II	AC	S	Pel	—15
3	50% Desorex HGD 4S + 50% Oxorbon K40J	Des-Oxo	AC	KI	Pel	—
4	50% DARCO H_2S + 50% CABOT RBHG4	Dar-Cab	AC	S	Pel, Par	—
5	Carbon foam	CF	C	None	Foam	20
3	IONEX Ag-400 B3 faujasite	IONEX	Z	Ag	Bead	21
7	Clariant AC-6120	AC-6120	A	Ag	Bead	22
8	Ag-functionalized aerogel	FA-Ag	AG	Ag	Par	8
9	Ag-xerogel	HTX-Ag	XG	Ag	Par	9
10	Reduced Ag-thiolated xerogel	HTX-S-Ag^0	XG	Ag, S	Par	9
11	Unreduced Ag-thiolated xerogel	HTX-S-Ag^+	XG	Ag, S	Par	9
12	75Ag_2S–PAN	PAN	P	Ag, S	Bead	23

Fig. 1 Optical images of the sorbent materials before iodine uptake.

were yellow/white or brown with different color gradations after iodine uptake, indicating the chemisorption of iodine to Ag and the formation of AgI.[10,11,17] Fig. 2b and c show the light yellow color changes in the upper areas of the HTX-Ag and AC-6210 sorbents due to AgI formation over time. The appearances of the activated carbons and carbon foam remained the same after iodine uptake.

The iodine loadings of all the sorbents were calculated using eqn (1) and (2), where m_s was the starting mass of the sample (see Table S1, ESI†), m_{s+I} is the final mass following iodine capture, m_I was the mass gain during the test (all gained mass was assumed as iodine), and q is the term denoting the mass of iodine captured per starting mass of the sorbent.

$$m_I = m_{s+I} - m_s \quad (1)$$

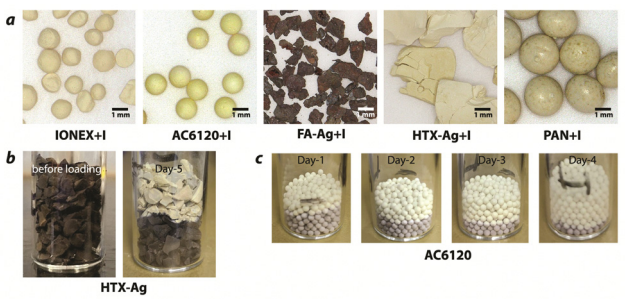

Fig. 2 Optical images of (a) Ag-containing sorbents after iodine uptake, (b) HTX-Ag before iodine loading and on 5 d, and (c) AC-6120 showing a color change as more iodine was loaded over 4 consecutive days.

$$q = m_I m_s^{-1} \text{ (mg g}^{-1}\text{)} \quad (2)$$

Table 2 shows the final iodine loading values before and after desorption, and Fig. 3 shows the iodine loadings over time. The CF sorbent gained ≈85% of its max loading after 1 d and plateaued the fastest; this is attributed to the small sample mass used (≈0.0205 g), porosity, and sorption mechanism. The Ag-thiolated xerogels, AC-6120, and PAN reached the equilibrium state in 7 d, 10 d, and 30 d, respectively. All the activated carbons, IONEX, and FA-Ag were still showing strong adsorption of iodine until the last day of iodine uptake before desorption. The results showed that the activated carbons had iodine loadings of 536–1165 mg g^{-1} after desorption, and the Des-Oxo sorbent showed the highest iodine loading. The changes in the q values of the activated carbons after 114 h of desorption were ≈7–15 mass% decrease due to the removal of weakly bonded or physisorbed species. As the desorption process is often slower than adsorption due to lower driving force, the reported desorption values of iodine only reflect the fraction of physisorbed iodine. Thus, considering all the iodine not desorbed as being chemisorbed may be an over representation of the quantities of chemisorbed iodine.

The Ag-containing xerogels had similar iodine loadings of 527–584 mg g^{-1} after desorption, whereas FA-Ag was at 394 mg g^{-1}. The change of q values for Ag-xerogels after

Table 2 Iodine loading of sorbents before (q_b) and after (q_d) desorption. Δ% shows the % change of q after desorption

#	Sorbents	q_b (mg g^{-1})	q_d (mg g^{-1})	Δ%
1	BAT37	950 ± 28	857 ± 45	−10
2	BAT37-II	630 ± 32	536 ± 28	−15
3	Des-Oxo	1249 ± 35	1165 ± 9	−7
4	Dar-Cab	746 ± 74	655 ± 83	−12
5	CF	734 ± 29	596 ± 19	−19
6	IONEX	479 ± 24	480 ± 19	0.2
7	AC-6120	87 ± 3	82 ± 3	−6
8	FA-Ag	485 ± 15	394 ± 11	−18
9	HTX-Ag	567	559	−1
10	HTX-S-Ag^0	603	584	−3
11	HTX-S-Ag^+	519	527	1.5
12	PAN	744	742	−0.3

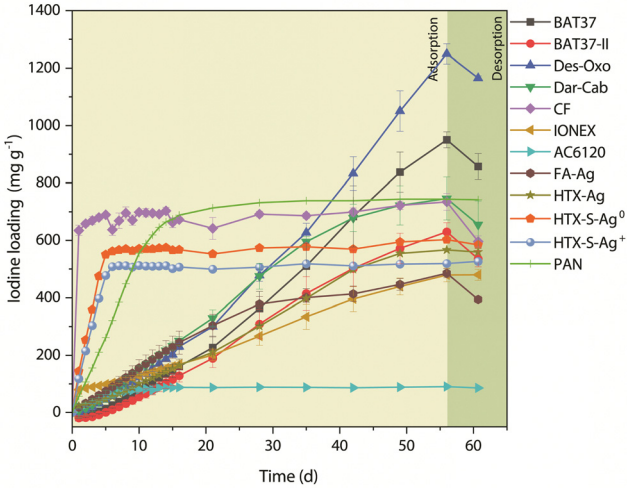

Fig. 3 Iodine loadings of sorbents for 56 d at 71 ± 2 °C followed by 4.7 d of desorption.

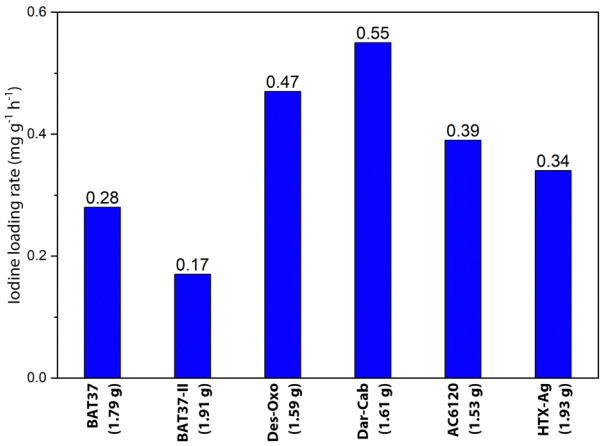

Fig. 4 Iodine adsorption rates of activated carbon (BAT37, BAT37-II, Des-Oxo, Dar-Cab), AC-6120 alumina, and HTX-Ag xerogel sorbents in the first 7 d of iodine uptake. The initial sample masses are given below the sample names.

desorption were relatively small (2–3 mass%) compared to activated carbons (≥7 mass%). The IONEX and PAN sorbents showed iodine loadings of 480 and 742 mg g^{-1}, respectively, with <0.3 mass% change after desorption, and these low changes potentially indicated the full chemisorption of iodine. The carbon foam sorbent had iodine loading of 596 mg g^{-1} and showed the highest decrease after desorption, *i.e.*, 19 mass%. The AC-6120 had the lowest iodine loading (82 mg g^{-1}) among the tested sorbents. Interestingly, BAT37 and BAT37-II lost mass in the first 3 and 4 days, respectively, and this mass loss was attributed to moisture loss or the cross interaction with other samples. Several additional experiments were performed to investigate possible cross reaction between sorbents including FA-Ag and IONEX (see Table S2 and Fig. S12, ESI†). The results showed that iodine loading for FA-Ag increased by 52% without desorption and 30% after desorption compared to values from the 56 d experiment. Similarly, iodine loading of IONEX also increased by 34% before desorption and 28% after desorption compared to the 56 d experiment. Further investigation should be performed in a future study to understand the cross reactions between different sorbents.

The iodine adsorption rates of the sorbents with similar initial masses (≈1.5–1.9 g) were calculated by linearly fitting the iodine loading values of the first 7 d (Fig. 4). The adsorption rates of the sorbents with low initial masses (≈0.02–0.30 g) were not compared as the resulting q values would be higher with similar iodine mass uptake due to these low initial masses, and this could be misleading. Among the compared sorbents, Dar-Cab showed the highest adsorption rate of 0.55 mg g^{-1} h^{-1}, and BAT37-II showed the lowest adsorption rate of 0.17 mg g^{-1} h^{-1} under the given conditions.

The structural changes before and after iodine uptake were analyzed using powder X-ray diffraction (PXRD). The sorbents were ground to a fine particle size and placed into the cavities of zero-background quartz holders (MTI Corp.). PXRD was performed using a Bruker D8 Advance diffractometer with a Cu tube between 10–55° or 10–70° 2θ with 0.02° or 0.03° 2θ steps and 1–3 s dwell time per step. Bruker AXS DIFFRAC EVA software was used to identify phases.

The XRD patterns of the sorbents before and after iodine uptake are shown in Fig. S1–S11 (ESI†). The XRD patterns of the as-received activated carbons showed two broad peaks around 25° and 44° 2θ indicating amorphous carbon structures, and a sharp peak around 26.7° 2θ attributed to quartz and/or a graphite phase.[24] All the activated carbons had sulfur-containing phases. The raw BAT37 sorbent contained Na_2SO_4 along with graphite and SiO_2 phases, but most of the crystalline phases decomposed except for a small peak of graphite after exposure to iodine at 71 °C for 56 d (Fig. S1, ESI†). The BAT37-II sorbent initially contained Na_2SO_4 and $CaSO_4$ phases along with graphite and SiO_2 phases, but after iodine uptake, only $CaSO_4$ and graphite phases were observed, along with a few small unidentified peaks (Fig. S2, ESI†). The Des, Oxo, Dar, and Cab sorbents showed the presence of graphite, SiO_2, and CaS before iodine uptake (Fig. S3 and S4, ESI†). The Des-Oxo sorbent showed an amorphous hump with small KI, graphite, and SiO_2 diffraction peaks after iodine uptake (Fig. S3, ESI†). The Dar-Cab sorbent had a small peak, which was identified as $CaCO_3$ (calcite), at ≈29.5° 2θ after iodine uptake (Fig. S4, ESI†). The CF sorbent was amorphous before and after iodine uptake (Fig. S5, ESI†).

The Ag-containing sorbents chemisorbed iodine and formed AgI phases during iodine uptake, which was observed in other studies.[9–11,16,17] The IONEX sorbent contained an Ag-faujasite phase before iodine uptake, and the faujasite crystal structure decomposed and formed β-AgI and γ-AgI phases after iodine uptake (Fig. S6, ESI†); this has also been seen in previous studies.[11,21] The FA-Ag and HTX xerogels were amorphous before iodine uptake and showed β-AgI and γ-AgI phases after iodine uptake (Fig. S7–S10, ESI†). The PAN composite contained Ag_2S before iodine uptake, and Ag_2S was collapsed and formed β-AgI and γ-AgI during iodine uptake (Fig. S11, ESI†).[23] The iodine-loaded activated carbons contained small crystalline peaks, which remain unidentified.

The range of q_d and Δ% values (see Table 2) between these sorbents as well as differing specific surfaces areas (active capture surfaces), capture mechanisms (*i.e.*, physisorption-based, chemisorption-based, or a combination thereof), costs, commercial availabilities, and volume-scale availabilities provide a cross-cutting list of potential options for iodine capture. While some of these are off-the-shelf solutions, other developmental (not currently commercially available) options might prove more effective at iodine capture under certain conditions. While a particular sorbent might show great promise, if it is not commercially available, implementing it at an industrial scale could take many years to realize. The set of experiments discussed comparing the performance of FA-Ag and IONEX show the interactions that certain sorbents might have and how mutualistic symbiotic effects might exist between separate sorbents where, when combined, they could capture more than the combination of each separately. This effect should be explored more in the future.

Three sorbents including HTX-S-Ag^0, HTX-S-Ag^+, and PAN reached the adsorption plateaus and were examined for their respective adsorption kinetics. The three data sets were fitted (Fig. 5) using the pseudo-first-order model [eqn (3)] after completing a nonlinear fit analysis through Mathematica[25] software. The value for q was taken to be the final value of q for each data set, and k is the rate constant (Table S3, ESI†). This indicates a higher initial concentration of adsorbate relative to active adsorption sites.[26]

$$q(t) = q_e\,(1 - e^{-kt}) \quad (3)$$

Summary and conclusions

Different sorbent materials, including six activated carbons, an aerogel, three xerogels, an alumina, a zeolite, and a carbon foam were investigated simultaneously for gaseous iodine loading at 71 °C for 56 d followed by 4.7 d of desorption. The iodine loadings of activated carbons were 630–1249 mg g^{-1} before desorption and decreased by 7–15% after desorption due to loss of weakly bonded or physisorbed species. All the Ag-containing sorbents chemisorbed iodine and formed AgI during iodine uptake. The Ag-xerogels had iodine loadings of 519–603 mg g^{-1} before desorption and lost <2% during desorption, whereas the Ag-aerogel with 485 mg g^{-1} before desorption lost ≈18% during desorption. The Ag-faujasite with 479 mg g^{-1} and Ag_2S–PAN composite with 744 mg g^{-1} were also stable during desorption. The Ag-alumina showed the lowest iodine loading of 87 mg g^{-1}. The tested commercial activated carbons with impregnated sulfur species, which are designed for Hg gas capture, showed their potential to be used as dual-functional sorbents to capture $I_{2(g)}$ and Hg vapors from off-gas systems in nuclear waste facilities. The developmental sorbents, including the Ag-xerogels and PAN composites, showed stable loading of iodine with little desorption, and their loading capacities with Hg will be investigated in a future study to evaluate their potential use as dual-functional sorbents for $I_{2(g)}$ and Hg vapors. When multiple sorbents are run simultaneously, this can lead to unexpected results; thus, samples should be run individually to evaluate individual performances. This is currently being done in a follow-up study to the current work.

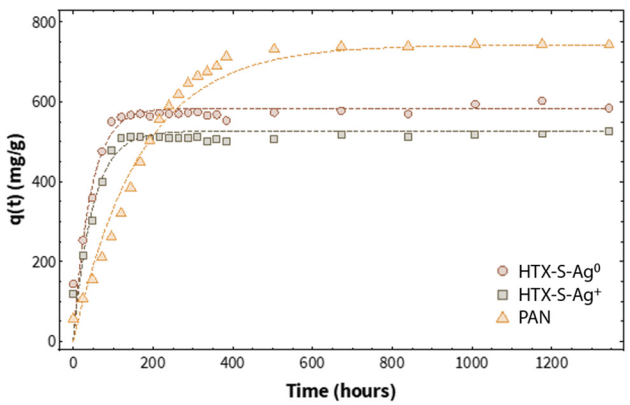

Fig. 5 Adsorption kinetic models for sorbents that reached adsorption plateaus.

This work was funded by the U.S. Department of Energy Office of Environmental Management. Pacific Northwest National Laboratory (PNNL) is operated by Battelle Memorial Institute for the DOE under contract DE-AC05-76RL01830. Contributions from Baskaran, Sullivan and Carlson were supported by the United States Department of Energy (DOE) Nuclear Energy University Program (NEUP) under contract DE-NE0008900, DOE Office of River Protection managed by Albert Kruger under contract 89304021CEM000014, and the US Nuclear Regulatory Commission (USNRC) under contract 31310022M015. The authors thank Josef Matyas for his help in producing the FA-Ag sorbent.

Author contributions

SC – data curation, investigating, methodology, writing – original draft. BJR – conceptualization, funding acquisition, data curation, investigation, visualization, methodology, writing – original draft, writing – review and editing. KB – data curation, investigating, methodology. SS – data curation, investigating, methodology. LEK – data curation, visualization, review, methodology. KC – conceptualization, data curation, investigation, methodology, writing – review and editing. MA – methodology, review. MF – funding acquisition, methodology, writing – review and editing.

Conflicts of interest

There are no conflicts to declare.

Notes and references

1 B. J. Riley, J. D. Vienna, D. M. Strachan, J. S. McCloy and J. L. Jerden Jr, *J. Nucl. Mater.*, 2016, **470**, 307–326.

2 R. T. Jubin, *A literature survey of methods to remove iodine from off gas streams using solid sorbents*, Oak Ridge National Laboratory, Oak Ridge, Tennessee, 1979.
3 L. L. Burger and R. D. Scheele, *HWVP Iodine Trap Evaluation*, Pacific Northwest National Laboratory, Richland, Washington, 2004.
4 E. M. Baum, H. D. Knox and T. R. Miller, *Nuclides and isotopes: chart of the nuclides*, KAPL Schenectady, NY, 2002.
5 S. Poncin, A.-C. Gérard, M. Boucquey, M. Senou, P. B. Calderon, B. Knoops, B. Lengele, M.-C. Many and I. M. Colin, *Endocrinology*, 2007, **149**, 424–433.
6 X. Hou, P. P. Povinec, L. Zhang, K. Shi, D. Biddulph, C.-C. Chang, Y. Fan, R. Golser, Y. Hou and M. Ješkovsky, *Environ. Sci. Technol.*, 2013, **47**, 3091–3098.
7 J. D. Vienna, E. D. Collins, J. V. Crum, W. L. Ebert, S. M. Frank, T. G. Garn, D. Gombert, R. Jones, R. T. Jubin and V. C. Maio, *Closed fuel cycle waste treatment strategy*, Pacific Northwest National Labatory, Richland, Washington, 2015.
8 J. Matyáš, E. S. Ilton and L. Kovařík, *RSC Adv.*, 2018, **8**, 31843–31852.
9 B. J. Riley, S. Chong, J. Marcial, N. Lahiri, M. K. Bera, S. Lee, T. Wu, K. Kruska and J. Matyáš, *ACS Appl. Nano Mater.*, 2022, **5**, 9478–9494.
10 S. Chong, B. J. Riley, J. A. Peterson, M. J. Olszta and Z. J. Nelson, *ACS Appl. Mater. Interfaces*, 2020, **12**, 26127–26136.
11 B. J. Riley, S. Chong, J. Schmid, J. Marcial, E. T. Nienhuis, M. K. Bera, S. Lee, N. L. Canfield, S. Kim, M. A. Derewinski and R. K. Motkuri, *ACS Appl. Mater. Interfaces*, 2022, **14**, 18439–18452.
12 F. Marrakchi, M. J. Ahmed, W. A. Khanday, M. Asif and B. H. Hameed, *Int. J. Biol. Macromol.*, 2017, **98**, 233–239.
13 W. A. Khanday, M. Asif and B. H. Hameed, *Int. J. Biol. Macromol.*, 2017, **95**, 895–902.
14 D. F. Sava, T. J. Garino and T. M. Nenoff, *Ind. Eng. Chem. Res.*, 2012, **51**, 614–620.
15 M. S. Fountain, R. M. Asmussen, B. J. Riley, S. Chong, S. Choi and J. Matyáš, *Mercury Abatement Materials Selection in Nuclear Waste Processing Off-Gas Streams*, Report PNNL-33818, RPT-EMTD-001, Pacific Northwest National Laboratory, Richland, WA, 2022.
16 S. Chong, B. J. Riley, W. Kuang and M. J. Olszta, *ACS Omega*, 2021, **6**, 11628–11638.
17 B. J. Riley, S. Chong and N. L. Canfield, *New J. Chem.*, 2024, **48**, 3352–3356.
18 K. Baskaran, M. Ali, B. J. Riley, I. Zharov and K. Carlson, *ACS Mater. Lett.*, 2022, **4**, 1780–1786.
19 A. Fujii Yamagata, S. A. Saslow, J. J. Neeway, T. Varga, L. R. Reno, Z. Zhu, K. A. Rod, B. R. Johnson, J. A. Silverstein, J. H. Westsik, G. L. Smith and R. M. Asmussen, *J. Environ. Radioact.*, 2022, **244–245**, 106824.
20 K. Baskaran, M. Ali, B. J. Riley, I. Zharov and K. Carlson, *ACS Mater. Lett.*, 2022, **4**, 1780–1786.
21 A. Yadav, S. Chong, B. J. Riley, J. S. McCloy and A. Goel, *Ind. Eng. Chem. Res.*, 2023, **62**, 3635–3646.
22 D. R. Haefner and T. J. Tranter, *Methods of Gas Phase Capture of Iodine from Fuel Reprocessing Off-Gas: A Literature Survey*, Report INL/EXT-07-12299, Idaho National Laboratory, Idaho Falls, ID, 2007.
23 B. J. Riley, S. Chong and N. L. Canfield, *New J. Chem.*, 2024, **48**, 3352–3356.
24 C. F. Ramirez-Gutierrez, R. Arias-Niquepa, J. J. Prías-Barragán and M. E. Rodriguez-Garcia, *J. Environ. Chem. Eng.*, 2020, **8**, 103636.
25 Wolfram Research, Inc. (www.wolfram.com), Mathematica Online, Champaign, IL, 2024.
26 J. Wang and X. Guo, *J. Hazard. Mater.*, 2020, **390**, 122156.

